Supplement of Observed changes in the temperature dependence response of surface ozone under NOx reductions

Noelia Otero, Henning W. Rust and Tim Butler

List of figures
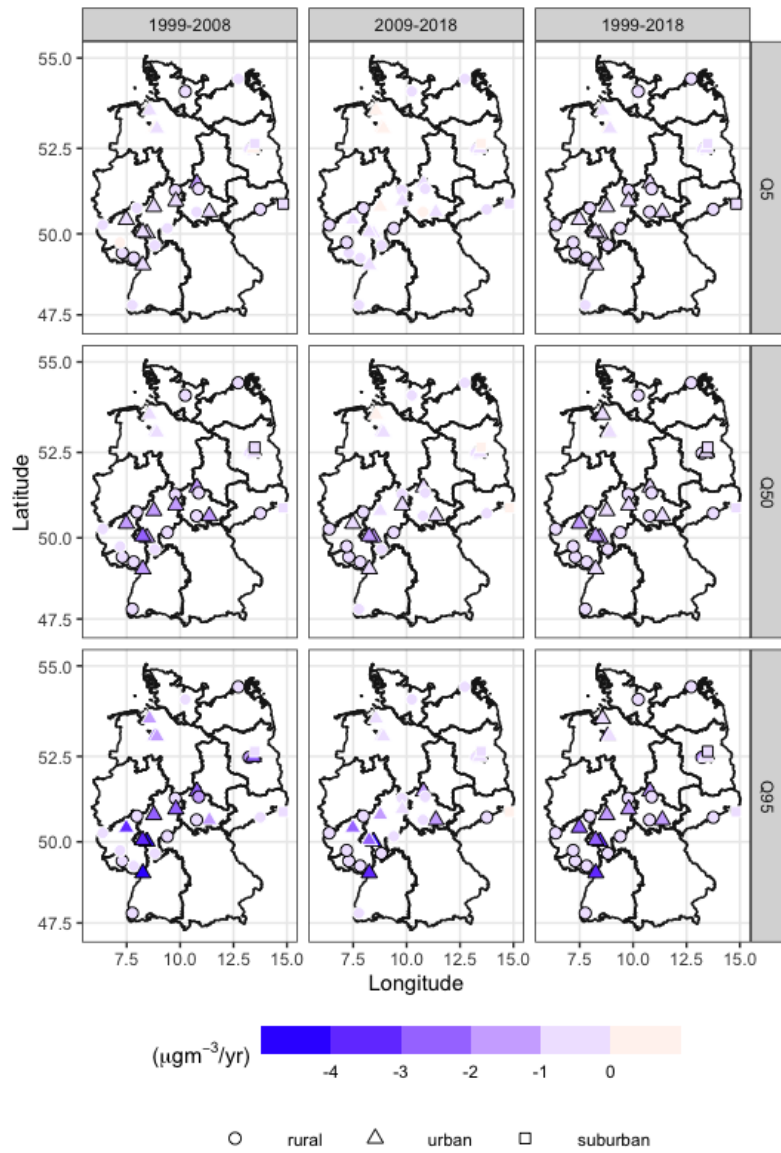
Figure S1. Spatial distribution of trends calculated separetely for each station and period, 1999-2008, 2009-2018, and the complete period 1999-2018
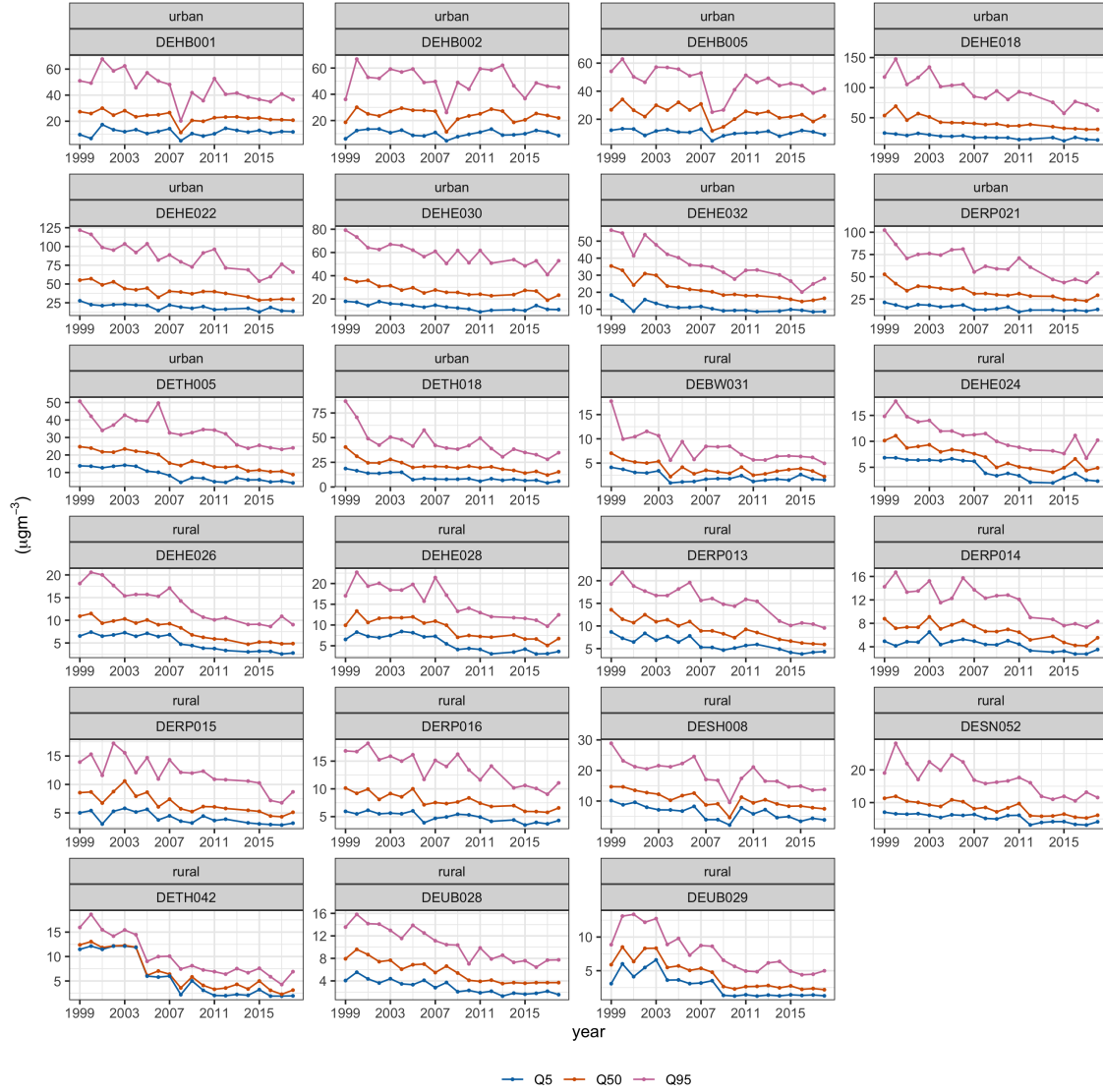
Figure S2. Time series of the annual 5th, 50th, 95th, percentiles for the rest of the urban and rural stations not presented in the main text
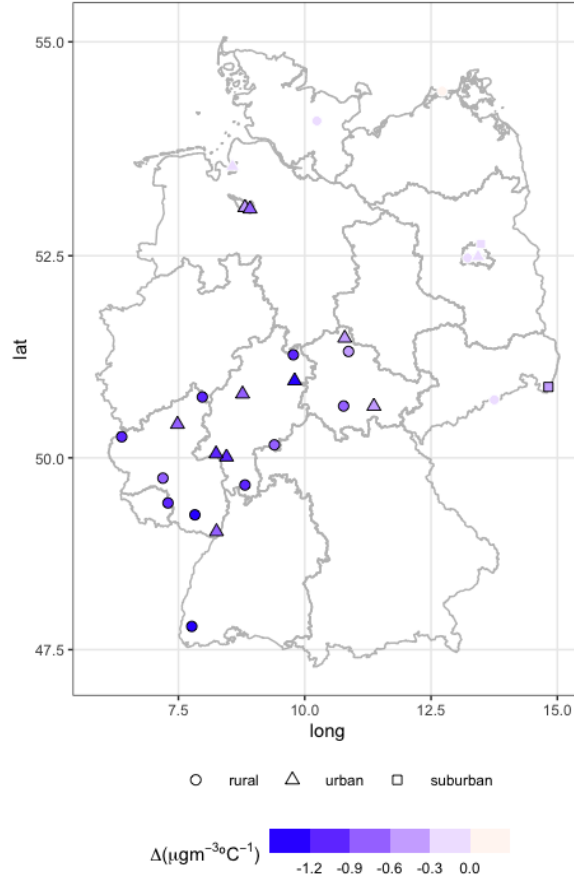
Figure S3. Spatial distribution of estimated differences in the slopes between the second period, 2009-2018, and the first period, 1999-2008
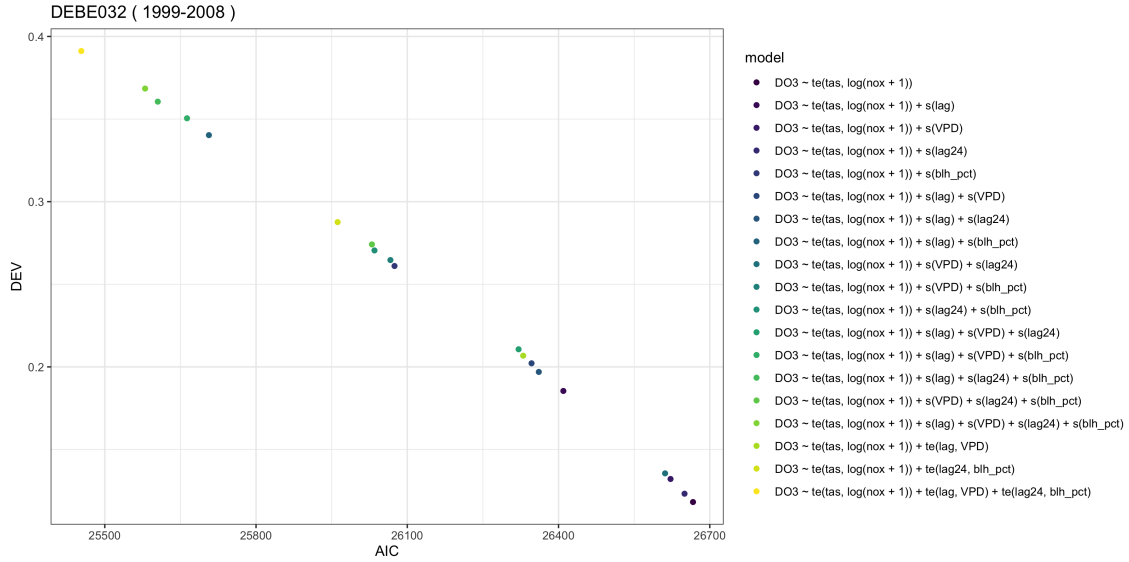
Figure S4. AIC and deviance explained (DEV) for each model used during the stepwise process at one rural station during the first period 1999-2008.
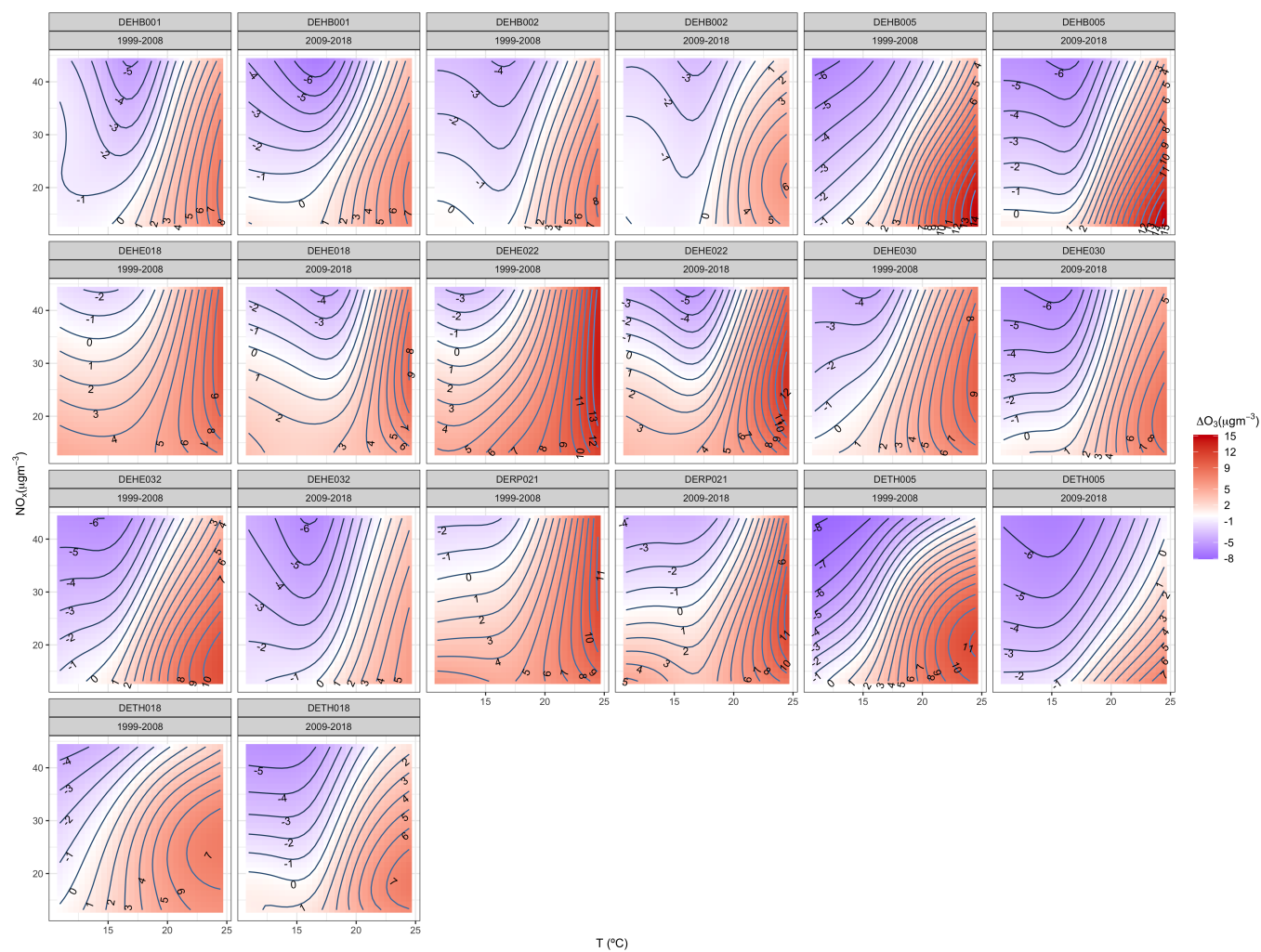
Figure S5. Countour plots obtained for the interaction term temperature and NOx from each GAMs built separetaly at each urban station and corresponding period.
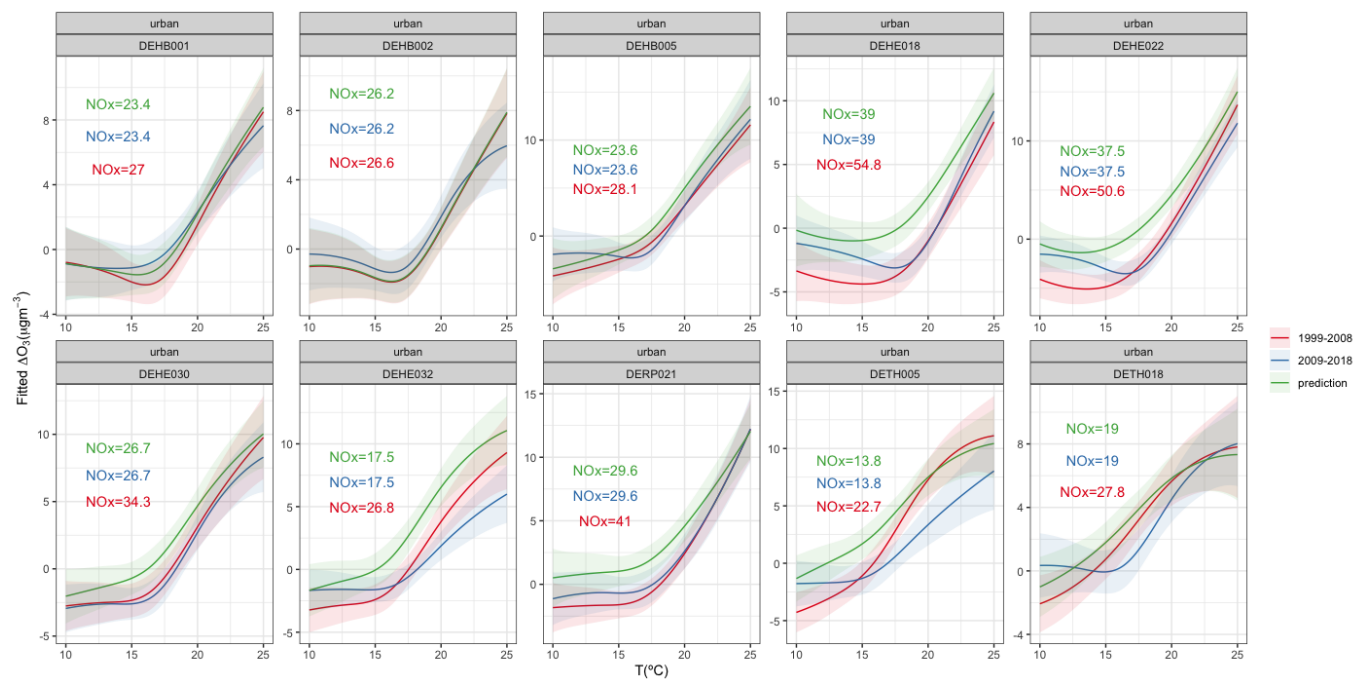
Figure S6. Estimated regression lines for urban stations of the ozone response to temperature while holding NOx concentrations constant (mean values for each period and station). Red line correspond to the prediction for the first period 1999-2008 (GAM-P1), blue line corresponds to the second period 2009-2018 and gree line corresponds to the projected response using GAM-P1 with mean NOx conditions of the second period. Shaded bands represent the pointwise 95% confidence interval.
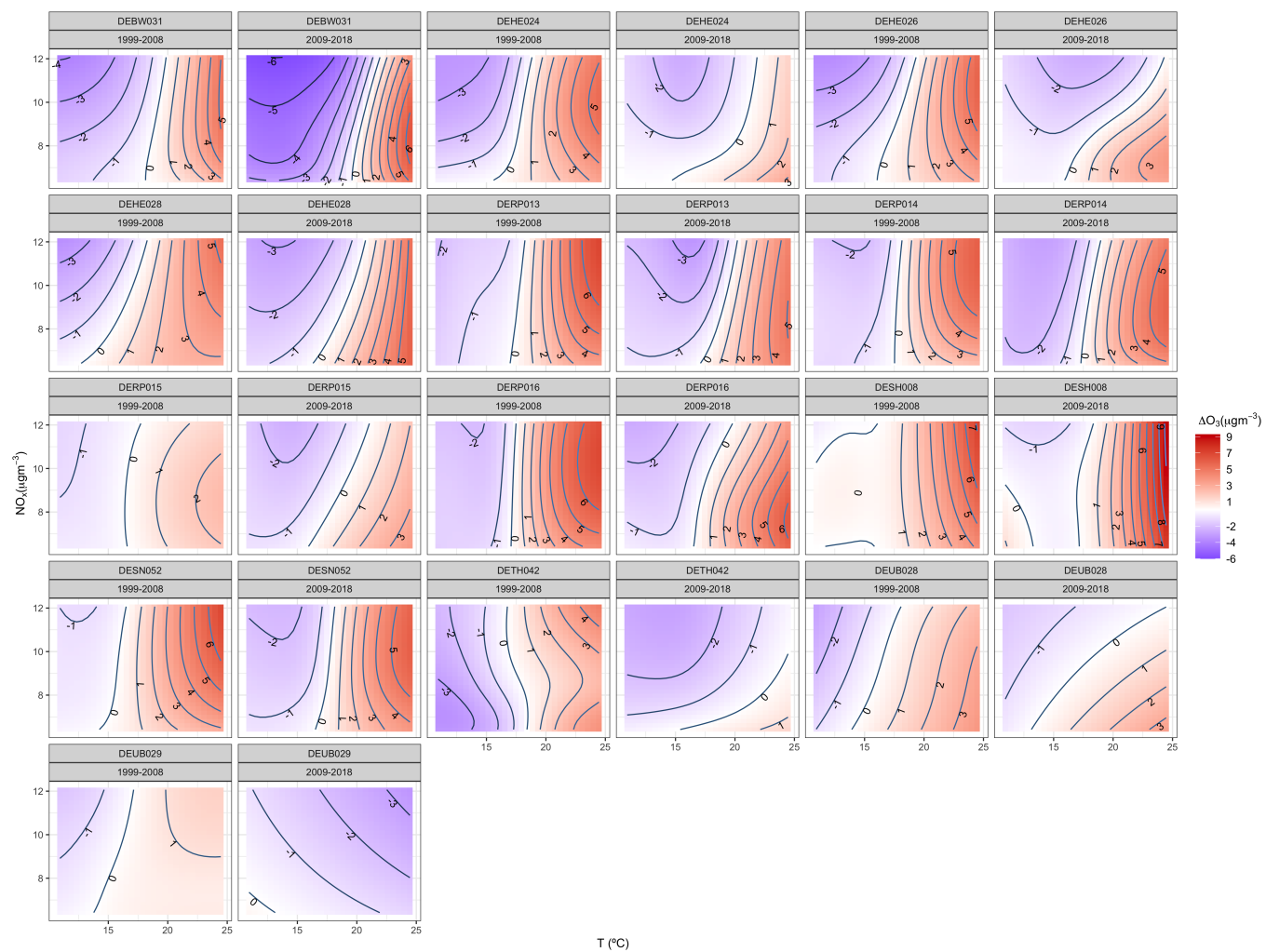
Figure S7. As Fig. S5, but for rural stations.
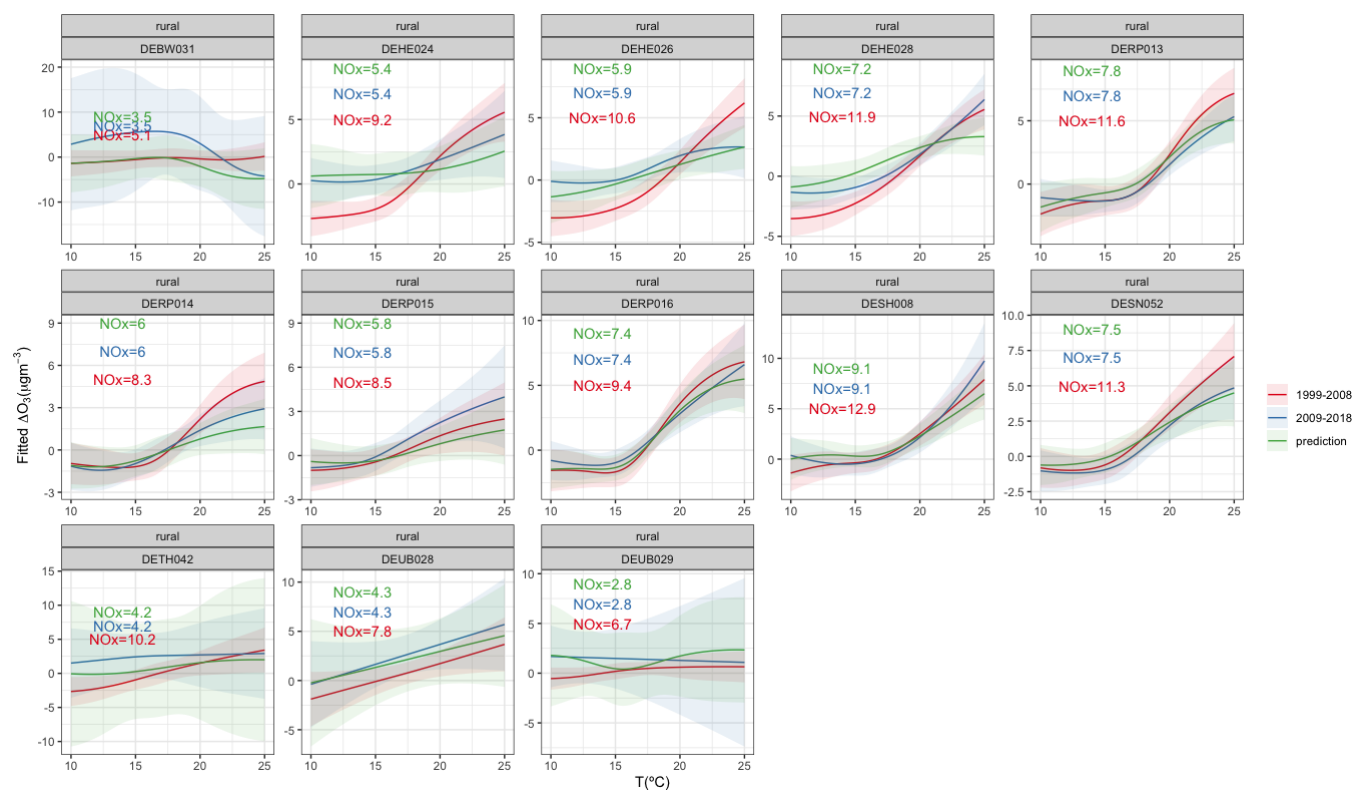
Figure S8. As Fig. S6, but for rural stations.
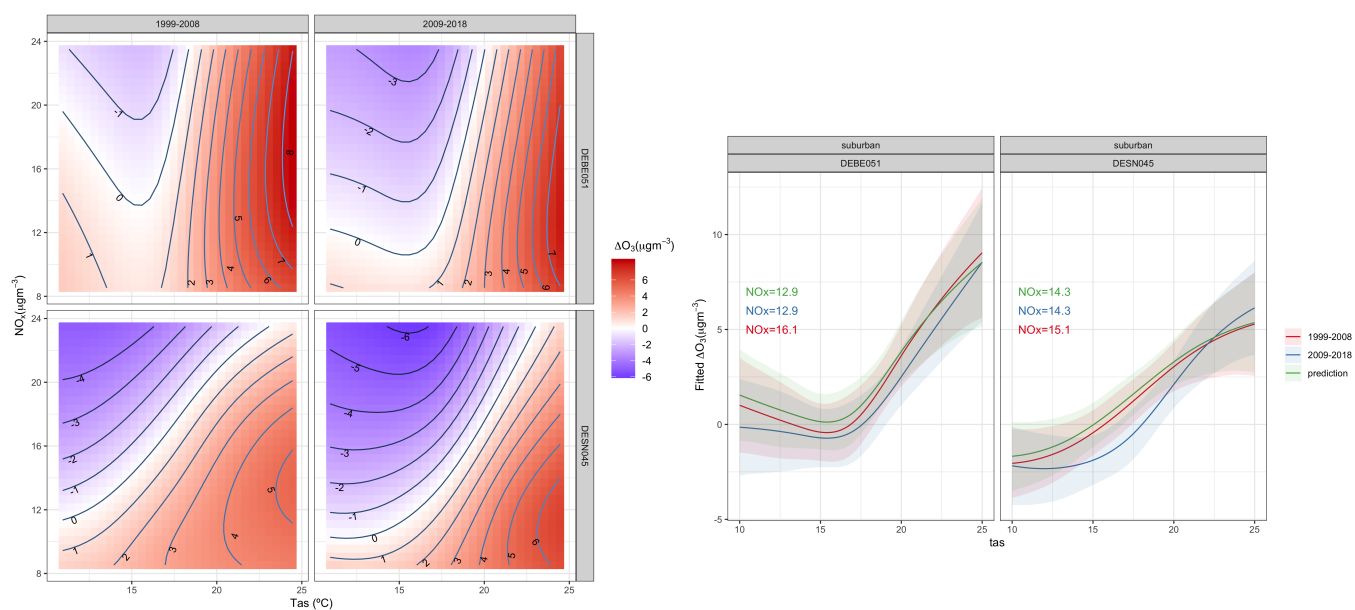
Figure S9. As Fig. 5 in the main text., but for the suburban stations.
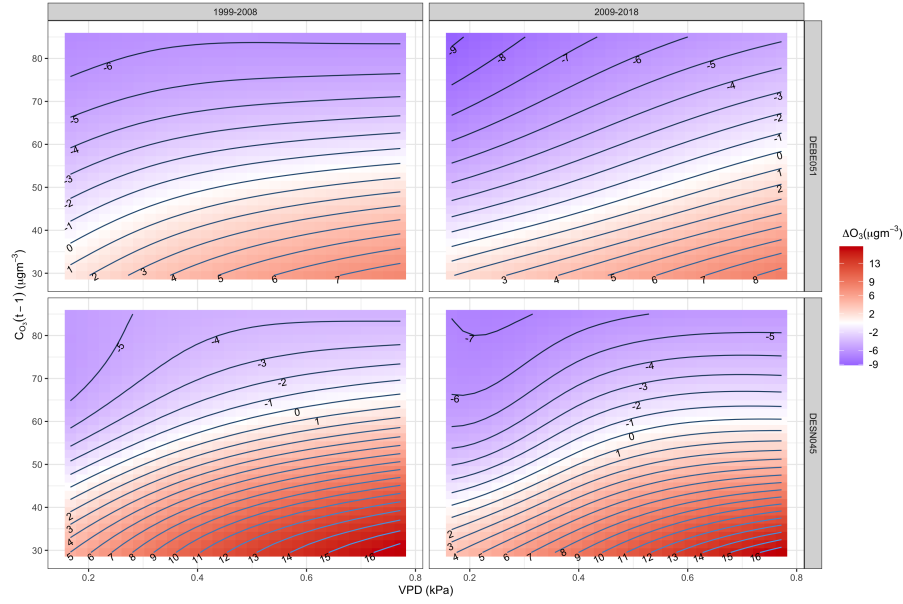
Figure S10. Contour plot for the interaction VPD-$C_{O_3}(t-1)$ at the suburban stations for the first period 1999-2008 and second period 2009-2018.
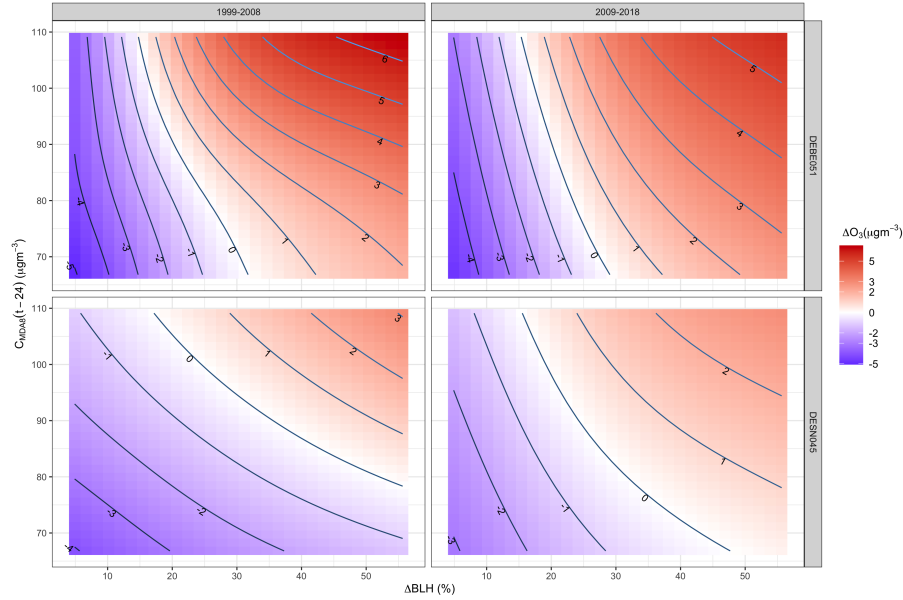
Figure S11. Contour plot for the interaction ΔBLH-$C_{MDA8}(t-24)$ at the suburban stations for the periods 1999-2008 and 2009-2018 at the suburban stations.